NanoImpact 29 (2023) 100452

Contents lists available at ScienceDirect

NanoImpact

journal homepage: www.elsevier.com/locate/nanoimpact

Gene expression profiling of human macrophages after graphene oxide and graphene nanoplatelets treatment reveals particle-specific regulation of pathways

Daria Korejwo [a,b], Savvina Chortarea [a], Chrysovalanto Louka [a], Marija Buljan [a], Barbara Rothen-Rutishauser [b], Peter Wick [a,1], Tina Buerki-Thurnherr [a,*,1]

[a] Particles-Biology Interactions Lab, Empa, Swiss Federal Laboratories for Materials Science and Technology, 9014 St. Gallen, Switzerland
[b] Adolphe Merkle Institute, University of Fribourg, 1700 Fribourg, Switzerland

ARTICLE INFO

Keywords:
Graphene-related materials
Transcriptomics
Macrophages
In vitro toxicity
Lung

ABSTRACT

Graphene and its derivatives are attractive materials envisaged to enable a wealth of novel applications in many fields including energy, electronics, composite materials or health. A comprehensive understanding of the potential adverse effects of graphene-related materials (GRM) in humans is a prerequisite to the safe use of these promising materials. Here, we exploited gene expression profiling to identify transcriptional responses and toxicity pathways induced by graphene oxide (GO) and graphene nanoplatelets (GNP) in human macrophages. Primary human monocyte-derived macrophages (MDM) and a human macrophage cell line, i.e. differentiated THP-1 cells, were exposed to 5 or 20 μg/mL GO and GNP for 6 and 24 h to capture early and more persistent acute responses at realistic or slightly overdose concentrations. GO and GNP induced time-, dose- and macrophage type-specific differential expression of a substantial number of genes with some overlap between the two GRM types (up to 384 genes (9.6%) or 447 genes (20.4%) in THP-1 or MDM, respectively) but also a high number of genes exclusively deregulated from each material type. Furthermore, GRM responses on gene expression were highly different from those induced by inflammogenic material crystalline quartz (maximum of 64 (2.3%) or 318 (11.3%) common genes for MDM treated with 20 μg/mL GO and GNP, respectively). Further bioinformatics analysis revealed that GNP predominantly activated genes controlling inflammatory and apoptotic pathways whereas GO showed only limited inflammatory responses. Interestingly, both GRM affected the expression of genes related to antigen processing and presentation and in addition, GO activated pathways of neutrophil activation, degranulation and immunity in MDM. Overall, this study provides an extensive resource of potential toxicity mechanisms for future safety assessment of GRM in more advanced model systems to verify if the observed changes in gene expression in human macrophages could lead to long-term consequences on human health.

1. Introduction

With the extensive use of nanomaterial (NM)-based products, the safety and sustainability of NM with attention to the potential impact on human health has become crucial. In the last years, great emphasis has been given to graphene and graphene-related materials (GRM) due to high expectations for the development of new technological applications in the fields of energy storage, nano-electronic devices, sensors, electronics, and biomedical applications (Wick et al., 2014). GRM are derivatives of monolayer graphene, and their classification is based mainly on three key parameters including the number of layers, the average lateral dimension and the atomic carbon oxygen (C/O) ratio. Defined by their properties, GRM can be either graphene oxide (GO) or few-layer graphene nanoplatelets (GNP) with micro- or nano-sized lateral dimensions (Wick et al., 2014). The scientific and technological interest in graphene increased rapidly when the physicists who produced graphene for the first time received the noble prize for their discovery (Novoselov et al., 2004; Geim and Novoselov, 2007). With the

* Corresponding author at: Empa, Lerchenfeldstrasse 5, 9014 St. Gallen, Switzerland.
E-mail address: tina.buerki@empa.ch (T. Buerki-Thurnherr).
[1] Shared last authorship.

https://doi.org/10.1016/j.impact.2023.100452
Received 11 August 2022; Received in revised form 9 December 2022; Accepted 19 January 2023
Available online 27 January 2023

emerging interest in GRM, the EU launched the largest scientific research initiative *Graphene Flagship* (www.graphene-flagship.eu, n.d.), assigned to take graphene from laboratories into the market, with a budget of €1 billion. With the rise in graphene and GRM production, the production volume has reached thousands of tonnes per year (Barkan, 2019). Several graphene technologies developed in laboratories have already been translated into commercial products, with applications in sports equipment, automotive coatings, or conductive inks (Kong et al., 2019). GRM are expected to enter the environment during the production, use and disposal of GRM-containing products. Consequently, human exposure to GRM is inevitable, with inhalation being the primary route of entry for GRM being released as an aerosol. Human exposure to airborne NM has been frequently associated with adverse health effects (Mühlfeld and Ochs, 2009; Oberdörster et al., 2007) and thus, safety of GRM needs to be confirmed before their widespread use or to implement safety measures at the working place. This is urgently needed considering the apparent conflicting findings of current literature on GRM in vitro and in vivo toxicity. While some studies reported that certain GRM induce oxidative stress, cell apoptosis or DNA damage (Li et al., 2018; Li et al., 2012; Akhavan et al., 2012; Liu et al., 2013) others did not find any adverse effects (Drasler et al., 2018; Schinwald et al., 2012; Schinwald et al., 2014; Mukherjee et al., 2018a) possibly due to differences in the experimental design (e.g., biological models, GRM materials, applied doses, exposure conditions).

The respiratory tract and in particular the sensitive gas-exchange region of the alveoli is highly susceptible to inhaled foreign particles and NM (Mühlfeld and Ochs, 2009; Oberdörster et al., 2007; Riediker et al., 2019). Prominent examples are micron-sized asbestos fibres and crystalline silica particles, which can induce a severe chronic inflammatory response and damages to the lung (Brunner et al., 2006; Donaldson et al., 2010; Warheit et al., 1984). To better understand the human health risks of pulmonary NM exposure, in vitro toxicity assessment can provide valuable mechanistic insights on NM interactions with key cell types of the air-blood tissue barrier. Macrophages are among the first and primary cells to process foreign particles and are central mediators of immune homeostasis and inflammatory responses (Hussell and Bell, 2014; Barlow et al., 2005). Several studies have shown that NM depositing in the respiratory part of the lungs are mainly found in alveolar macrophages (Barlow et al., 2005; Brown et al., 2019). This includes also GRM, which have been shown to accumuate in alveolar tissues and macrophages after inhalation exposure in rodents (Shin et al., 2015; Creutzenberg et al., 2022). In a previous study we investigated the impact of different GRM with distinct physicochemical properties on acute toxicity responses (48 h) in differentiated THP-1 macrophages (Netkueakul et al., 2020). Although all GRM induced the formation of intracellular reactive oxygen species (ROS) we only observed oxidative stress and inflammatory responses as well as cytotoxicity for one type of large graphene nanoplatelets (GNP) and only at high concentrations (20 and 40 μg/mL). However, the molecular events leading to the observed toxicity of GNP are largely unknown. Moreover, the previously investigated acute toxicity endpoints might not reveal more subtle effects of GRM on macrophage functionality.

Here, we aimed to achieve an in-depth insight on the molecular mechanisms and pathways triggered by GO and GNP in human macrophages. Moreover, we performed transcriptome profiling in human primary monocyte derived macrophages (MDM) as well as in differentiated THP-1 macrophages to assess if this widely used cell line (Chanput et al., 2014) can deliver predictive responses. Primary cells are considered to better reflect physiological responses than cell lines, which could be particularly relevant for transcriptomic profiling of NM effects. A comprehensive understanding of GRM bio-responses at the molecular level will be highly valuable for risk assessment and management of GRM.

2. Materials and methods

2.1. Materials

The GNP and GO materials used in this study were from commercial sources (GNP from XG Science, USA; GO from Cheaptubes, USA) and have been extensively characterized in our previous study (Netkueakul et al., 2020). A summary of the GO and GNP characteristics is provided in Table 1. Crystalline quartz particles (DQ) were included as an inflammatory benchmark control and were purchased from Dörentrup Quartz GmbH & Co. KG (material No. 04; mean particle diameter d(50) = 3.71 μm, d(97) = 12.03 μm). To remove possible endotoxin contaminations in the material, both GO and GNP powders were heated at 80 °C for 4 h.

The materials were characterized and used in a previous study (Shin et al., 2015) and a summary is provided here. AFM, atomic force microscopy; SEM, scanning electron microscopy; NA: not applicable (PdI >0.7); PBS, phosphate buffered saline; PdI: polydispersity index; XPS, x-ray photoelectron spectroscopy. [(a)] Value from manufacturer; [(b)] AFM measurements performed in (Netkueakul et al., 2020); [(b)] Intensity ratio of D- to G-bands determined by Raman spectroscopy measured at 532 nm in (Netkueakul et al., 2020).

2.2. Cell culture and cell treatment

Human THP-1 monocytes were obtained from the European collection of cell cultures (Lot number13 C011, ECOCC). Following thawing, cells were grown in suspension in 75 cm^2 cell culture flasks (TPP), subcultured at least three times prior to experiments and grown in complete cell culture medium (RPMI-1640 medium, Sigma-Aldrich) supplemented with 10% foetal calf serum (FCS, Sigma-Aldrich), 1% L-glutamine (Sigma-Aldrich) and 1% penicillin–streptomycin–neomycin (PSN, Sigma-Aldrich). Cells were maintained at 37 °C and 5% CO_2 in a humidified atmosphere and routinely sub-cultured twice a week. For experiments, THP-1 monocytes were differentiated to macrophages with 200 nM phorbol 12-myristate 13-acetate (PMA; Sigma-Aldrich) for 72 h before GRM exposure. THP-1 cells were seeded in 12 well plates at densities of 5×10^5 cells per well (3.9 cm^2 growth area) in 1000 μL complete cell culture medium and cultivated for 72 h in the presence of 200 nM PMA. After differentiation, PMA containing medium was removed and the cells were washed with pre-warmed phosphate buffered saline (PBS) twice before experiments.

Peripheral blood was obtained from 7 donations from 4 donors under informed consent according to approval from the local cantonal ethics committee, St. Gallen, Switzerland (BASEC Nr. PB_2016–00816). Monocytes were isolated from blood provided by health donors as described by Sallusto et al. (Sallusto et al., 1995; Blank et al., 2011) with the modification of using CD14 magnetic beads (MicroBeads, Miltenyi Biotec) for monocyte isolation. The primary monocytes were seeded in 6-well plates with densities of 1×10^6 cells per well in 2000 μL complete

Table 1
GRM characterization data.

Material type	GO	GNP
Lateral Dimension (SEM)	1–50 μm	5–150 μm
Number of layers or thickness (AFM)	Few to single layer[(a)] 21.6 ± 21.1 nm[(b)]	6–8 nm[(a)] 239 ± 174 nm[(b)]
Z_{ave} diameter (nm)/ PdI ± SD in water	765 ± 17.1 nm/ 0.42 ± 0.03	NA
Z_{ave} diameter (nm)/ PdI ± SD in medium	940 ± 87.7 nm/ 0.55 ± 0.04	NA
Raman I(D)/I(G) ratio [(a)]	0.94	0.52
C/O ratio (XPS)	1.8	33.5
Zeta potential in 10%PBS (mV) ± SD	−45.8 ± 2.93	−49.6 ± 3.65
Endotoxin contamination (80 μg/mL)	<0.011 EU/mL	0.015 EU/mL

cell culture medium and were differentiated into MDM with addition of 10 ng/mL macrophage colony stimulating factor (M-CSF, Miltenyi Biotec, Germany) in complete cell culture medium for 6 days. After differentiation cells were washed with prewarmed PBS twice before experiments. For all experiments, stock dispersions of the tested materials of 1 mg/mL in ultrapure water (GO) or sterile filtered (0.22 μm filter) 160 ppm Pluronic F-127 (Sigma-Aldrich) in ultra-pure water (GNP) were prepared by sonication for 10 min (ultrasonic bath, Sonorex Super RK 156 BH, Bandelin) prior to usage and used for maximum one month. Stock dispersions were diluted to the final experimental concentrations of 5 and 20 μg/mL in complete cell RPMI. DQ was freshly dispersed in H_2O, vortexed 1 min and applied with a final concentration of 100 μg/mL in complete cell culture medium.

2.3. RNA isolation

After the 6 h and 24 h treatment, material exposed, and control cells were collected in RNA protect buffer (QIAGEN). Total RNA was extracted using the miRNeasy® Mini kit (QIAGEN) according to the manufacturer's protocol. DNase digestion has been performed by RNase Free DNase Set (QIAGEN) to discard residual DNA contamination. The RNA samples were carefully labelled and stored at −80 °C prior to sequencing.

The quantity and quality of the RNA was determined with a Nanodrop ND-1000 (Thermo Fisher) and a Fragment Analyzer standard sensitivity RNA measurement (SS RNA kit (15 nt), Agilent, Waldbronn, Germany). The measured concentrations (> 200 ng/μL) and RIN (>8) values qualified for a Poly-A enrichment strategy to generate the sequencing libraries applying the TruSeq mRNA Stranded Library Prep Kit (Illumina, Inc., California, USA). After Poly-A selection using Oligo-dT beads the mRNA was reverse-transcribed into cDNA. The cDNA was fragmented, end-repaired and poly-adenylated before ligation of TruSeq UD Indices (IDT, Coralville, Iowa, USA). The quality and quantity of the amplified sequencing libraries were validated using a Fragment Analyzer SS NGS Fragment Kit (1–6000 bp) (Agilent, Waldbronn, Germany). The equimolar pool of 72 samples was sequenced on a NovaSeq6000 S1 FlowCell (Novaseq S1 Reagent Kit, 100 cycles, Illumina, Inc., California, USA) targeting ~10-15 M single reads per sample. The conversion to FastQ was performed using bcl2fastq2 v2.19 from the CASAVA software suite allowing for 0,1 mismatches per barcode. The quality scale used was Sanger/phred33/Illumina 1.8 + .

The RNA sequencing data associated with this publication have been deposited in ArrayExpress database and are accessible via the ArrayExpress E-MTAB-10099 series accession number.

2.4. Sequencing data analysis

Quality control checks including analysis of sequence quality, GC content, presence or contamination with adaptors, duplication levels and overrepresented sequences was conducted with FastQC (within Supporting User for SHell-script Integration (SUSHI)) (Hatakeyama et al., 2016; Andrews, n.d.-a; Andrews, n.d.-b). Processed sequencing reads were aligned against the human reference genome *Homo Sapiens* GRCH38 (Schneider et al., 2017; Chaisson et al., 2015) Spliced Transcripts Alignment to a Reference (STAR) software (Dobin et al., 2013; Dobin and Gingeras, 2016) which is extracting splice junctions from files and uses them to greatly improve accuracy of the mapping with STAR-app within SUSHI. Subsequently, CountQC was used as a quality check for the alignment (Anders and Huber, 2010). The read counts to genes were created using featureCounts (Anders and Huber, 2010; Liao et al., 2014).

2.5. Bioinformatics analysis

Differently expressed genes (DEG) between different treatments were determined with DEseq2 from the read counts. Only significantly differentially expressed genes with adjusted p-values <0.05 compared to untreated cells (neg. control) were considered for further analysis. Of note, DEseq2 adjusted p-values correspond to FDR-corrected p-values. For this, transcript abundances were quantified with the Kallisto software tool (Bray et al., 2016). Counts per transcript estimated this way were imported into R using the tximport package and information on gene-transcript relationships was obtained from the GRCh38 genome build. GRCh38 annotations were downloaded from the Ensembl database (Zerbino et al., 2018). Measurements were grouped per condition, i.e., the applied material, cell type and a time point. DESeq2 performs an internal normalization where geometric mean is calculated for each gene across all samples. Measurements for each material that were obtained at a specified time point (6 h or 24 h) were compared to the corresponding negative control measurements for the same time and cell type, i.e., all the analyses were performed separately for macrophages derived from THP-1 or from primary cells. For each condition (i.e., material and time point), R package DESeq2 was used to identify genes whose expression levels significantly differed from the corresponding levels in negative control. Only genes that had at least 1 count in the assessed conditions were considered further in the analyses. In order to assess distances among the compared gene expression measurements, the count data was first transformed with the variance stabilizing transformation (Anders and Huber, 2010), which is implemented in DESeq2, and the samples were grouped according to the values for the two main principal components. Genes were defined as differentially expressed if the adjusted p-value reported by DESeq2 was lower than 0.05 (fold change was not included as a criteria for the results shown here).

Clustering of measured samples was performed using the 'complete linkage' method implemented in the pheatmap R package. For this, distances among samples were calculated with the PoiClaClu R package and expression values (i.e., counts) of all genes were used. The package implements the Poisson Distance for calculating sample distances (Witten, 2011). It accounts for the Poisson distribution of RNAseq counts and takes the inherent variance structure of counts into consideration. Venn-diagrams were plotted with the webtool "VENNY 2.1" (https://bioinfogp.cnb.csic.es/tools/venny/) (Oliveros, n.d.). Enriched BioPlanet pathways (Huang et al., 2019) and gene ontologies were evaluated with the webtool EnrichR (Kuleshov et al., 2016; Chen et al., 2013). In addition, identification and visualization of the interactions and biological networks among the proteins encoded by DEGs annotated with the enriched functional terms and pathways were performed using the web-based Search Tool for the Retrieval of Interacting Genes (STRING) prediction platform (Szklarczyk et al., 2017).

2.6. qRT-PCR

RNA samples were transcribed into cDNA with the iScript™ cDNA Synthesis Kit (BIORAD). The resulting cDNA was subjected to real time PCR analysis on a CFX96 Dx (BIORAD) using the reaction volume containing 50 ng cDNA, iQ™ SYBR® Green Supermix (BIORAD), distilled H_2O and each primer pair was added at a final concentration of 200 nM. The relative gene expression of *BCL-2, FGR* and *IFI30* genes was evaluated. Primers were designed with Primer-BLAST based on the sequences accessible in NCBI. Gene expression levels were normalized to the housekeeping gene *GAPDH*. The primer sequences and cycling parameters are listed in Table S1. The qPCR data were analysed using the relative gene expression (ΔΔCT) method (Livak and Schmittgen, 2001).

2.7. Statistics

Results are presented as mean ± standard deviation (SD) of at least 3 independent experiments ($n = 3$). Statistical analysis was performed by a student's t-test and/or one-way ANOVA followed by Bonferroni's post-correction, using the software GraphPad Prism (version 9.0). The results were considered significant if $p < 0.05$.

3. Results and discussion

3.1. Characteristics of GRM and experimental design

Two types of GRM with distinct physicochemical properties (size, number of layers, C/O ratio) were selected based on our previous acute toxicity screening study including five different GRM in differentiated THP-1 macrophages (Netkueakul et al., 2020). The chosen commercial GO and GNP materials showed the most distinct response with GNP being more cytotoxic to THP-1 macrophages than GO after 24 h exposure to 40 μg/mL (MTS assay: 48% viability for GNP (significant reduction) and 102% for GO; LDH assay: significant 3.1 fold increase for GNP and 1.6 fold increase for GO) (Netkueakul et al., 2020). For the current study, we aimed to target an exposure relevant dose as well as a higher but still sub-lethal concentration representing a potential worst-case scenario. Due to the lack of GRM workplace exposure data, realistic concentrations for the dosage of GRM in occupational exposure settings were estimated from the current thresholds of carbon nanotubes (CNT) exposure. For CNT, a full working lifetime exposure would result in an alveolar mass retention of 10–50 μg/cm^2 and acute respiratory exposure (24 h) would be in the range of 1 μg/cm^2 (Drasler et al., 2018; Graham et al., 2017). Therefore, we chose 1.3 μg/cm^2 (5 μg/mL) and 12.5 μg/cm^2 (20 μg/mL) as low and high exposure concentrations. We have previously shown that 5 μg/mL GNP and GO were not cytotoxic to differentiated THP-1 cells after 24 h of exposure and only at 20 μg/mL, GNP but not GO induced a slight but non-significant effect (MTS assay: viability 100% for 20 μg/mL GO, 81.8% for 20 μg/mL GNP relative to untreated control; LDH assay: 1.1 fold increase for 20 μg/mL GO, 2.1 fold increase for 20 μg/mL GNP compared to untreated control) (Netkueakul et al., 2020).

These GRM have been extensively characterized and a summary of their properties is provided in Table 1. For the transcriptomic profiling study, we exposed primary MDM and THP-1 macrophages to GO or GNP at the low concentration of 5 μg/mL and the high concentration of 20 μg/mL for 6 h and 24 h (Fig. 1).

DQ silica particles served as toxic and well-characterized benchmark material with expected inflammogenic responses (Brunner et al., 2006; Clouter et al., 2001). In a pilot screening, we examined the pro-inflammatory dose-response (indicated by the release of interleukin-8 (IL-8)) of DQ in differentiated THP-1 cells and chose the concentration of 100 μg/mL for subsequent transcriptome profiling studies. At this concentration, DQ induced the secretion of IL-8 without affecting cell viability (Fig. S1A-B). By choosing two time points, we aimed to distinguish early, probably more general stress related responses (6 h) from GRM specific acute responses (24 h). After cell harvest and RNA isolation, RNA sequencing and bioinformatics analysis was performed to evaluate the differentially expressed genes and deregulated biological processes and pathways in response to GRM.

3.2. GRM induce specific and reproducible responses in differentiated THP-1 macrophages and MDM

All samples passed the raw data quality control checks and we further assessed if gene expression profiles reflected treatment to various materials. For this, we performed hierarchical clustering analysis using expression levels of all measured genes. The clustering indicated that different materials (GO, GNP and DQ) induced specific and reproducible responses in both macrophage types after 6 h (data not shown) and 24 h of treatment (Fig. 2). In differentiated THP-1 macrophages, replicates clustered clearly according to the treatment and dose. MDM samples also clustered well considering that samples originated from four individual donors.

3.3. GRM impact gene expression in a highly cell type-, time-, dose- and material-dependent manner

For each treatment, we identified genes with a significant expression change compared to non-treated cells (adjusted p-value <0.05). The number of genes with non-zero read counts that went into the DE analysis ranged from 15,810 to 16,428. The percentages of significant hits ranged from 0.01% (DQ after 6 h in MDM) to 17.8% and 17.5% (GO 5 μg/mL and GNP 20 μg/mL after 24 h in THP-1 cells). RNA-sequencing revealed that both GRM induced a considerable number of up- and downregulated genes in THP-1 macrophages and MDM (Figs. S2, S3, S4).

A first comparison of DEGs in dependence of the different macrophage types (i.e. differentiated THP-1 macrophages versus MDM) revealed a relatively low percentage of overlapping DEG for the low GRM treatment (5 μg/mL) at both time points (6 h and 24 h) (Fig. S2A). A considerably higher amount of overlapping DEGs in THP-1 macrophages and MDM was observed for the high GRM exposure (20 μg/mL) after 24 h (GO: 576 (46.9%) and 118 (12.4%) shared down- and up-regulated DEGs, respectively; GNP: 222 (12.2%) and 267 (13.9%) shared down- and up-regulated DEGs, respectively) (Fig. S2B). For the reference material DQ, the number of shared down- and up-regulated genes between the two macrophage types after 24 h of exposure was 4 (1.3%) and 74 (18.4%), respectively (Fig. S3). Further analyses was continued for both cell types to better understand differences and

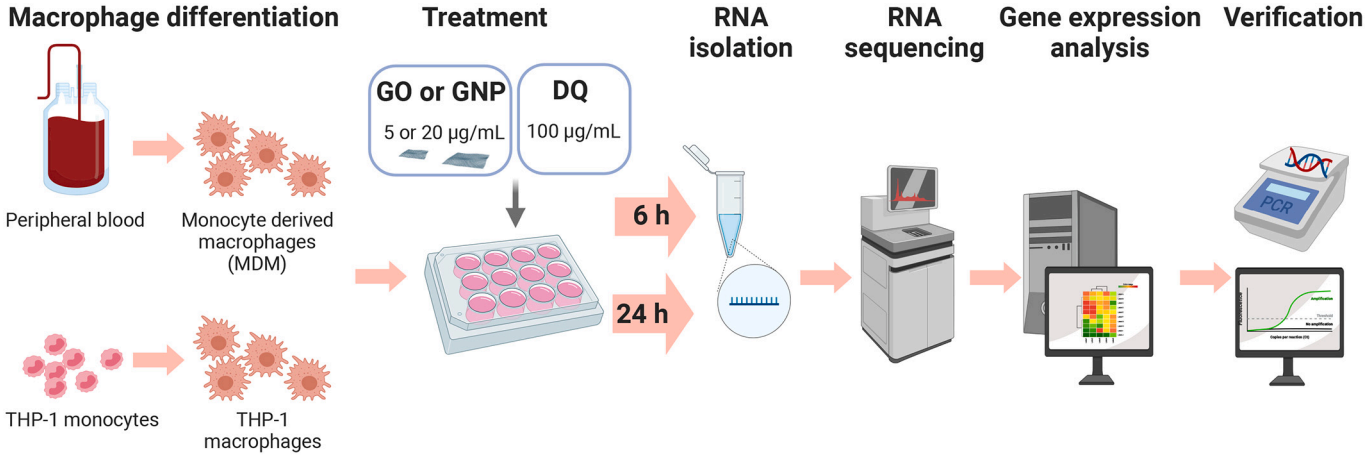

Fig. 1. Experimental setup. Human macrophages were isolated and differentiated from peripheral blood monocytes or differentiated from the THP-1 monocyte cell line. Cells were exposed to GO or GNP at concentrations of 5 and 20 μg/mL. Global transcriptomic responses were investigated after 6 h or 24 h of GRM exposure. DQ was used as positive reference material at a concentration of 100 μg/mL. Illustrations in Fig. 1 were created using http://BioRender.com.

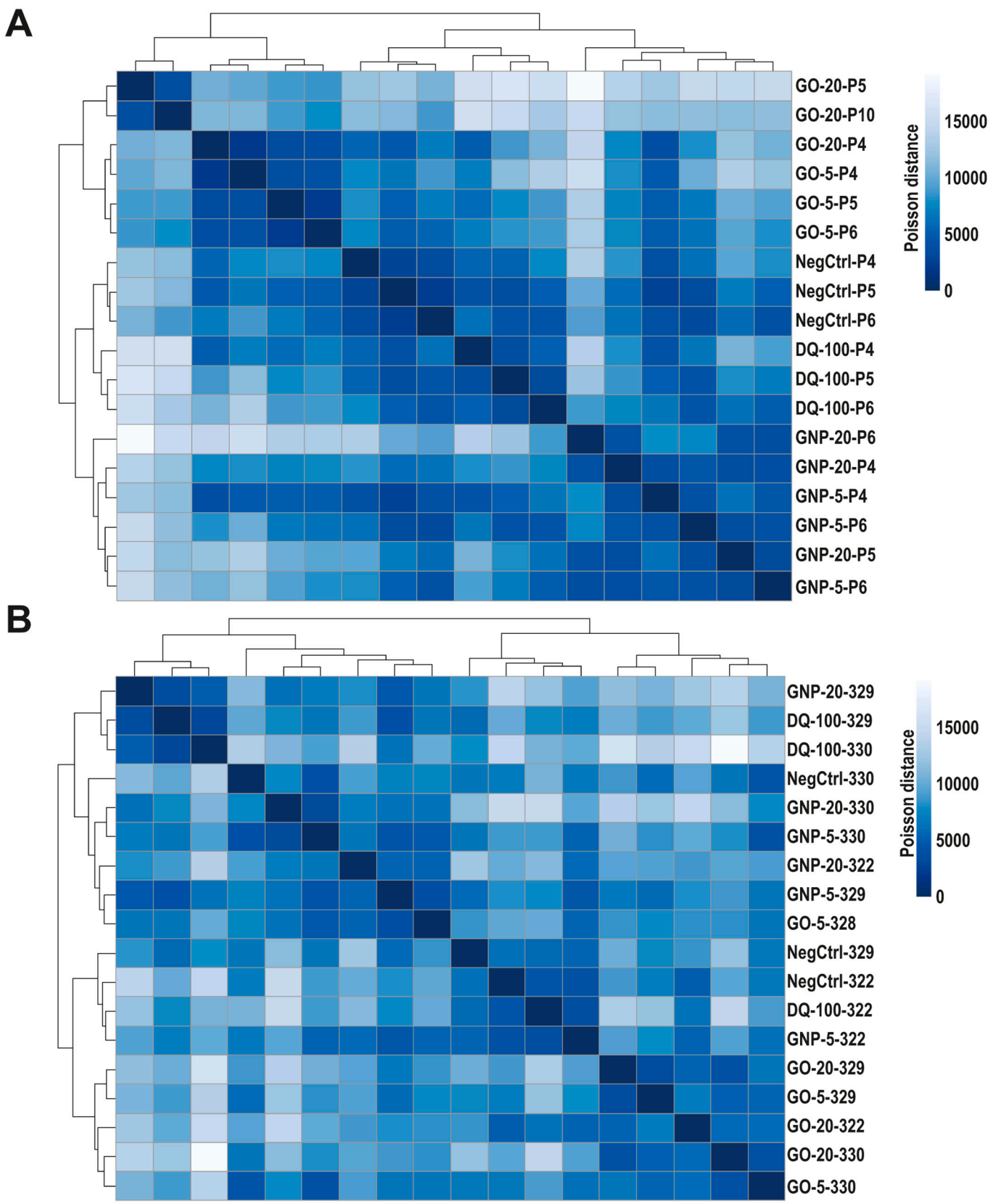

Fig. 2. Hierarchical clustering analysis of THP-1 and MDM samples. Correlation matrix with hierarchical clustering analysis of THP-1 macrophages (A) and MDM (B) treated with different concentrations of GO, GNP and DQ for 24 h or untreated (NegCtrl). The name of the sample is formed by combining the information about treatment, dose (μg/mL) and passage number (for THP-1 macrophages) or donor number (for MDM).

similarities in their response to GRM.

When comparing the time-response, both GRM induced a higher amount of DEG after 24 h compared to 6 h treament in THP-1 macrophages (Fig. S4A). In MDM, this trend was also observed for GO with the exception of a higher number of upregulated genes at 6 h of exposure to 5 μg/mL GO (Fig. S3B). However, GNP showed a more pronounced response at the early time point (6 h) in MDM. The amount of shared genes between the two time points ranged from 0.7 to 52.7% indicating the induction of fast sustained responses in gene expression (6 h and 24 h) in addition to fast transient (6 h only) and delayed (24 h only) responses.

In addition, there was a clear dose-response with the high GRM concentration of 20 μg/mL GRM inducing a more pronounced impact on gene regulation compared to the lower 5 μg/mL exposure dose in both cell types (Fig. S5). An inverse dose-response was only observed for THP-1 exposed to GO for 24 h.

Focusing on material-specific responses we found that for the two GRM, the number of shared DEG was between 8 (1.5%) to 384 (9.6%) in THP-1 cells and 3 (0.4%) to 447 (20.4%) in MDM with a larger overlap at the higher concentration (20 μg/mL) (Fig. 3). However, a considerable amount of DEG was unique to GO and GNP treatments. For instance, exposure at to 20 μg/mL GO for 24 h resulted in 1018 (25.4%) or 1214 (43%) unique genes in THP-1 cells or MDM, respectively while treatment with 20 μg/mL GNP for 24 h resulted in 2361 (59%) or 899 (31.9%) unique genes in THP-1 cells or MDM, respectively. The overlap between GO and DQ was below 45 genes (1.4%) for all investigated time points and doses in both cell types while the number of shared DEG between GNP and DQ was slightly higher in MDM after 24 h of exposure (98 genes/12.9% and 270 genes/9.6% at 5 or 20 μg/mL GNP, respectively). Only a very low amount of genes (≤ 48 genes or 1.7%) was commonly differentially expressed by all three materials.

In summary, there is a considerable number of DEGs uniquely deregulated from each material type indicating highly material-specific responses. This is probably not surprising since GRM are a group of materials with a broad range of distinct physicochemical properties (e.g., lateral dimension, number of layers, C/O ratio, presence of metal contaminants), which may lead to different biological responses. For example, a previous inhalation study in mice found that GO exposure induced a larger response on gene expression in lung and liver tissue than rGO (Poulsen et al., 2021). In addition to the distinct responses between GO and GNP, also the overlap with DQ was minimal, suggesting that the genes affected by GRM are probably not associated to silicosis toxicity related pathways. To further understand which biological processes and pathways are involved and whether the genes affected by GO and GNP are part of different biological processes or pathways, we performed further gene ontology enrichment and pathway analysis.

3.4. 3.3 GNP affect biological processes and pathways related to inflammation and apoptosis while GO and GNP interfere with genes involved in immune responses

For gene ontology and pathway analysis, we only focused on the 24 h time point since this was expected to reveal material-specific responses. Moreover, only the high exposure dose of 20 μg/mL GRM was included due to the stronger transcriptional responses (Fig. S5). Cell responses to GO and GNP exposure as assessed by EnrichR included biological processes associated with regulation of apoptosis, immune related responses, cellular processes and response to stimulus and metabolic processes (Fig. 4). Specifically, GO induced an up-regulation of genes involved in immune responses in MDM, as well as down-regulation of genes involved in translation in both macrophage types. GNP exhibited a strong up-regulation of inflammatory responses, along with down-regulation of translational and cell-cycle processes in both MDM and THP-1 macrophages. Additionally, GNP induced apoptotic signalling pathways and downregulated genes involved in antigen processing and presentation in MDM. As expected, the reference material DQ elicited a strong activation of genes involved in cytokine responses both in THP-1 macrophages and MDM (Fig. S6).

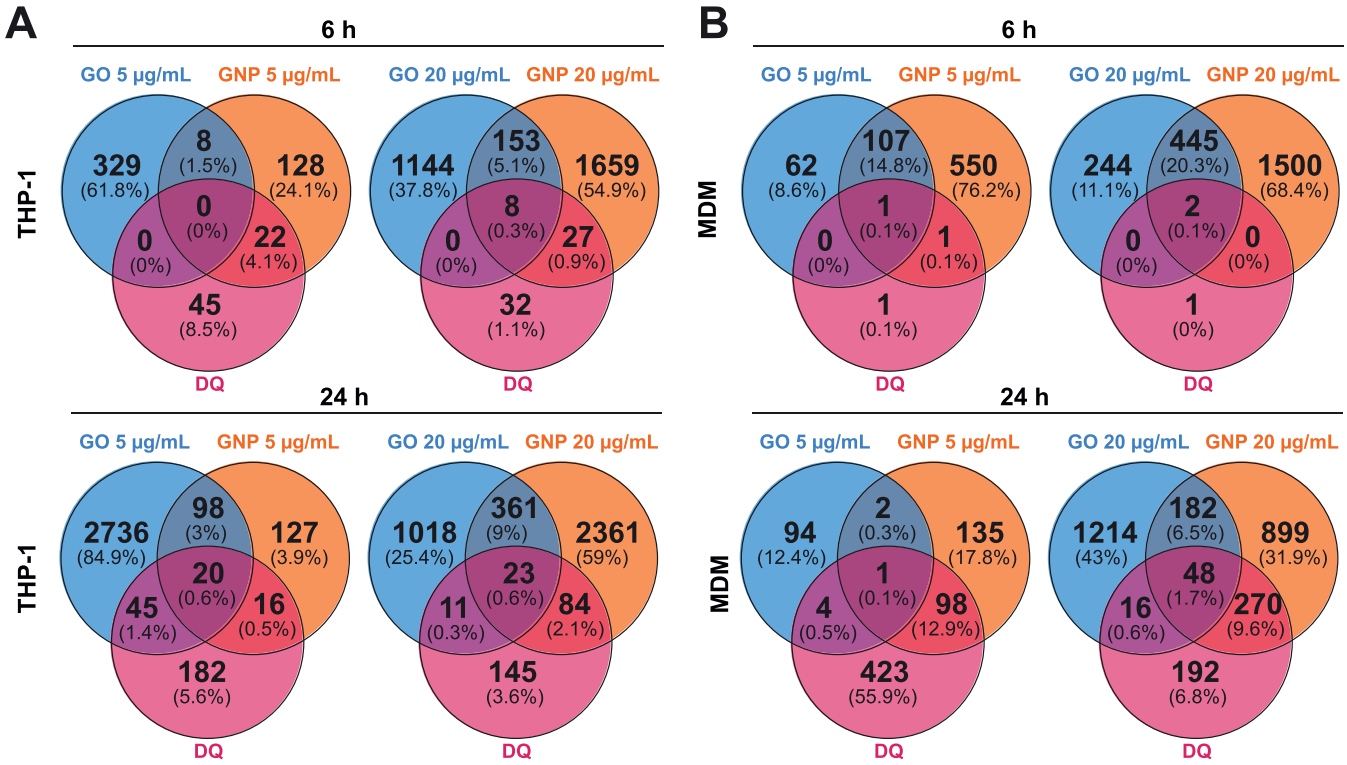

Fig. 3. VENN diagrams of DEG indicating material-specific responses in THP-1 macrophages and MDM. Comparison of DEG after 6 and 24 h of exposure to 5 or 20 μg/mL GO or GNP or 100 μg/mL DQ in THP-1 macrophages (A) or MDM (B).

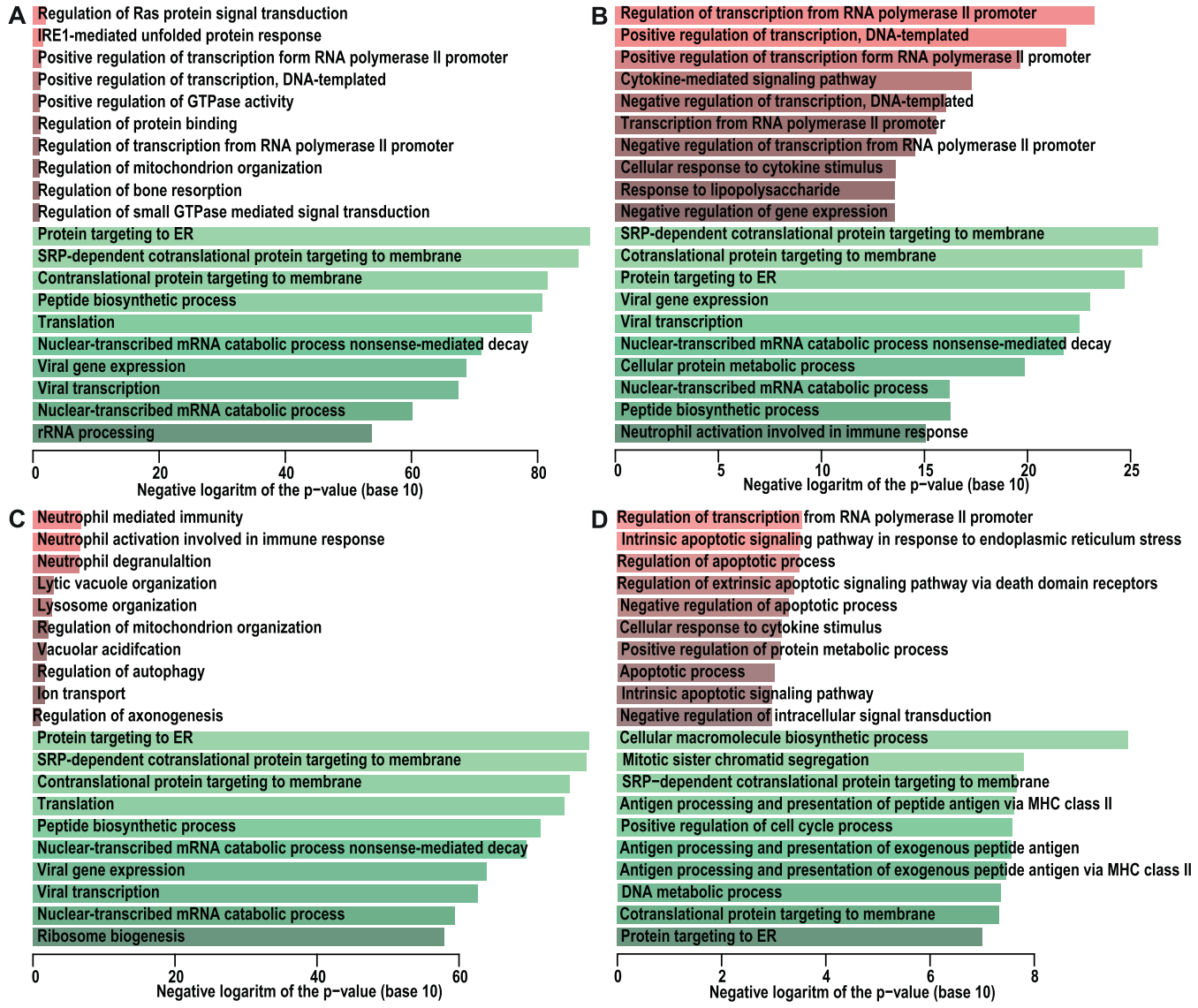

Fig. 4. Gene Ontology enrichment analysis. Top ten biological process terms significantly enriched with DEGs in THP-1 macrophages (A, B) and MDM (C,D) treated with 20 μg/mL GO (A, C) or GNP (B,D) for 24 h. The graphs represent up-regulated (red) and down-regulated (green) gene ontologies in each functional category. Bars are sorted by log of the *p*-value corrected for multiple testing. A full list of the enriched GO terms and the involved genes is available from Supplementary Table S2. (For interpretation of the references to colour in this figure legend, the reader is referred to the web version of this article).

Inflammatory responses have been previously described for various carbon-based NMs including GRM. For instance, single-walled carbon nanotubes (SWCNT) have been shown to trigger inflammation in primary macrophages and GO activated the inflammasome in these cells at similar NM concentrations and timepoints of 24 and 48 h or exposure (Mukherjee et al., 2018a; Mukherjee et al., 2018b; Scala et al., 2018). We observed pronounced changes in gene regulation involved in inflammatory pathways mostly for GNP but not GO treated macrophages. This is in line with results from our previous study, where we observed significant induction of IL-8 and IL-1β secretion in THP-1 macrophages after treatment with GNP but not GO (Netkueakul et al., 2020). Similar to our observations of negligible inflammatory responses of GO, Mukherjee et al. described pronounced effects on chemokine-encoding genes in MDM exposed to SWCNTs, but not in response to GO after 24 h exposure at concentrations up to 30 μg/mL (Mukherjee et al., 2018b). In contrast, Orecchioni et al. found that exposure to small GO sheets had a more significant impact on immune cells (human peripheral blood mononuclear cells) compared to large GO sheets, which was reflected in the upregulation of critical genes in immune responses and the release of cytokines IL1-β and TNF-α (Orecchioni et al., 2016). The absence of inflammatory responses of GO in our study might therefore be explained by the comparably large size of the investigated GO (1–50 μm) compared to the two GO materials (1–10 μm) used by Orecchioni and colleagues. Moreover, another study described size-independent effects of GO on inflammasome activation in primary human macrophages (Mukherjee et al., 2018a). Therefore, size is likely not the only factor that impacts on GRM bio-responses, but a combination of particle properties should be considered as recently evidenced in a multi-hierarchical structure activity relationship (SAR) assessment visualizing the contributions of seven basic properties of Fe_2O_3 (e.g. surface area and reactivity, hydrodynamic size, zeta-potential, aspect ratio) to its diverse bio-effects in THP-1 cells and animal lungs (Cai et al., 2018).

An interesting observation was that six out of the top 10 most enriched up-regulated gene ontology terms in GNP-exposed MDM were associated with the regulation of apoptotic processes (GO: 0070059, GO:0042981, GO:2001237, GO:0043066, GO:1902041, GO:0006915, GO:0097193). Subsequently, we searched the interactions among the DEGs involved in the apoptosis-related gene ontology terms and used

the web-based tool STRING to construct a protein interaction network (Fig. 5 A, B). Proteins encoded from the enriched genes are represented with nodes. To limit the number of observed interactions and to avoid false positive interactions, the settings were set to only identify gene expression with a "medium to high confidence" (score > 0.4). The thickness and opacity of each interaction line indicates the degree of confidence prediction for the interaction. A total of 112 interactions were obtained using 84 nodes among the analysed apoptotic-related genes. The *BCL-2* gene, a potent regulator of cell death with a crucial role in development, tissue homeostasis and immunity (Czabotar et al., 2014), exhibited high score interaction and its expression was further analysed by RT-PCR in both THP-1 and MDM after exposure to GO or GNP (5 and 20 μg/mL) for 24 h. A concentration-dependent increase (non-significant, $p > 0.05$) in *BCL-2* expression levels was detected after GO treatment in THP-1 and MDM as well as in GNP-treated THP-1 cells. A notable upregulation of *BCL-2* was also shown in GNP-treated MDM at 5 μg/mL. While we did not observe GRM-induced cytotoxicity on THP-1 cells or MDM, it remains to be investigated whether the observed changes in *BCL-2* expression could affect tissue homeostasis and immunity over prolonged exposure times.

Among the most highly ranged downregulated biological processes following GNP treatment in MDM were gene ontology terms related to antigen processing and presentation (GO:0002474, GO:0019886, GO:0002478). The constructed protein-protein interactions of a set of DEGs related to antigen processing revealed a dense network of 26 nodes and 96 edges. A leading role in this network was ascribed for *IFI30, a* novel mediator involved in immune processes but also in neutralization of ROS, maintaining the oxidative stress balance (Cacialli et al., 2021; Liu et al., 2020). An upregulation of *IFI30* expression (non-significant $p > 0.05$) was shown only in THP-1 cells after both GRM treatments but not in MDM (Fig. 5C). Therefore, other genes might be more relevant and further candidates from this network should be explored to

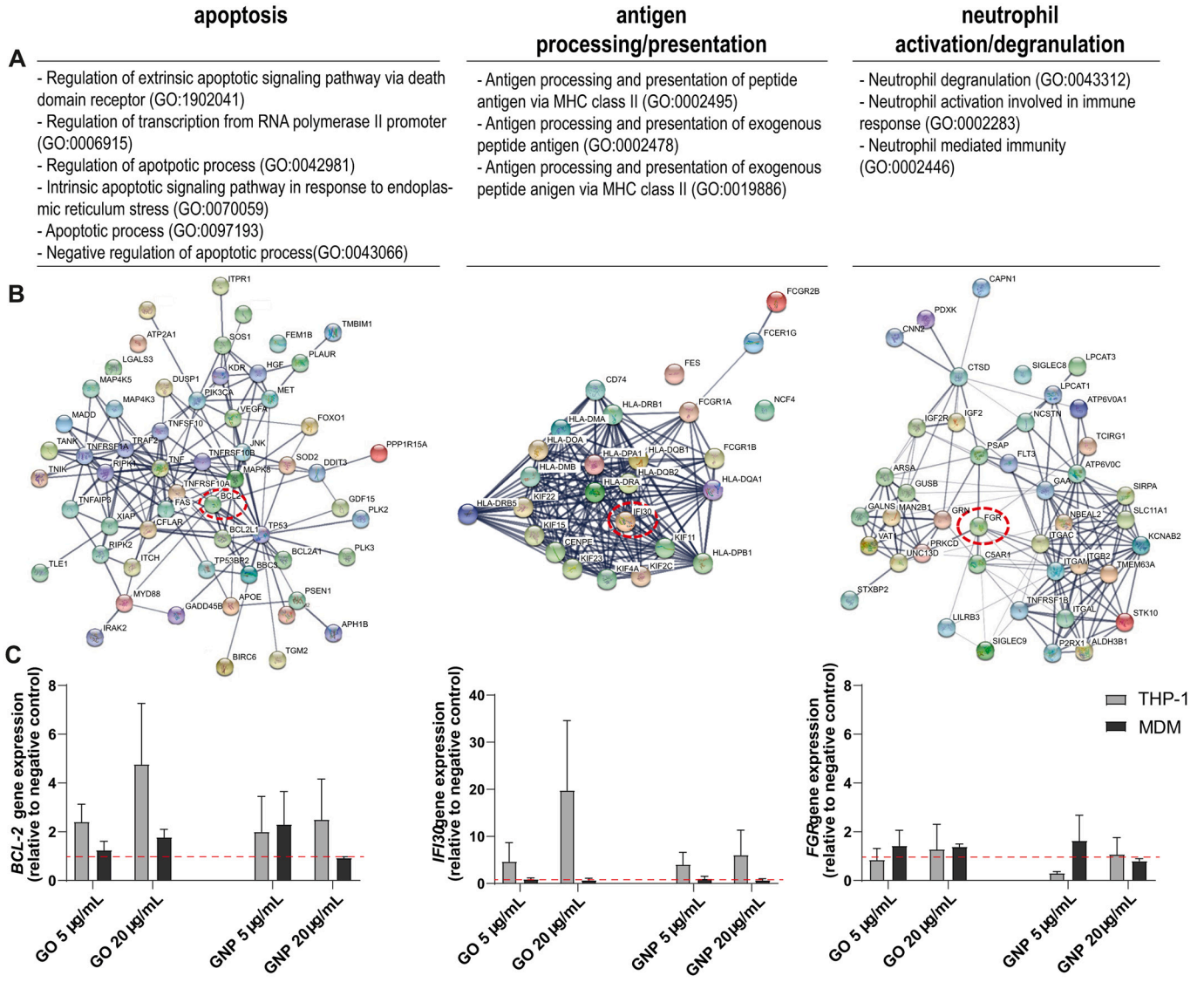

Fig. 5. Network analysis and RT-PCR validation of selected genes. (A) Highly enriched biological processes from GO enrichment analysis related to apoptosis, neutrophil activation/degranulation and antigen processing/presentation are indicated in the respective tables. (B) The list of differentially expressed genes in the GO biological processes was subjected to network analysis using STRING. The network includes the specific genes (nodes) enriched in the selected biological process respectively. The connections (edges) between the gene nodes represent physical, predicted, and genetic interactions but also shared protein domains and protein pathways. Coloured nodes indicate their engagement in different pathways of the relevant biological processes. The red dashed circle indicates the enriched gene of each network (*BCL-2*, *IFI30* and *FGR*) chosen for RT-PCR expression quantification. (C) THP-1 macrophages and MDM were treated with 5 or 20 μg/mL of GO or GNP and analysed at 24 h time-point. The relative gene expression levels were normalized to the untreated control and the housekeeping gene *GAPDH*. (For interpretation of the references to colour in this figure legend, the reader is referred to the web version of this article).

understand better how GNP may potentially perturb antigen processing and presentation in macrophages.

In addition, GO-associated top-ranked, enriched gene ontologies included neutrophil related biological pathways such as neutrophil degranulation (GO:0043312) neutrophil activation involved in immune response (GO:0002283) and neutrophil mediated immunity (GO:0002446). String network analysis resulted in 43 nodes and 56 edges indicating direct (physical) and indirect (functional) associations between the proteins encoded from the enriched genes (Fig. 5B). A key role in this network was attributed to *FGR*. FGR is a part of the largest family of protein kinases, the SRC family kinases (SFKs), and engages in the regulation of crucial cellular events i.e., cellular movement, differentiation, proliferation, survival, apoptosis and immune regulation (Jing et al., 2021; Tuguzbaeva et al., 2019). Changes in *FGR* expression after treatment with GRM in both macrophage types at 24 h revealed a significant upregulation of *FGR* in GO-treated MDM at high concentration (20 μg/mL) and a notable but insignificant increase ($p > 0.05$) at the low GO concentration of 5 μg/mL (Fig. 5C). Therefore, future studies on the impact of GO on immune processes related to neutrophil degranulation and activation are warranted. In fact, a recent in vivo transcriptomics study in mice exposed to GO by a single intratracheal instillation described increased expression of genes encoding neutrophil chemoattractants (e.g. *TNFα, CXCL5, SAA3,* and *CCL7*) associated with neutrophil infiltration in bronchoalveolar lavage (BAL) fluid (Poulsen et al., 2021).

Analysis of the top 10 up- and down-regulated pathways underlying GRM responses in THP-1 and MDM macrophages using EnrichR showed that up-regulated pathways were rather distinct between GO and GNP (Fig. 6). While GNP activated several immune-related pathways (related to IL-1, IL-2, IL-5 and TNF-α) and BDNF signalling pathway in both macrophage types, as well as p53 pathway in MDM, only the IL-2 signalling pathway was induced by GO in MDM. In contrast, GO strongly up-regulated chaperon and unfolded protein response (UPR) pathways in THP-1 macrophages and the lysosome pathway in MDM. UPR was

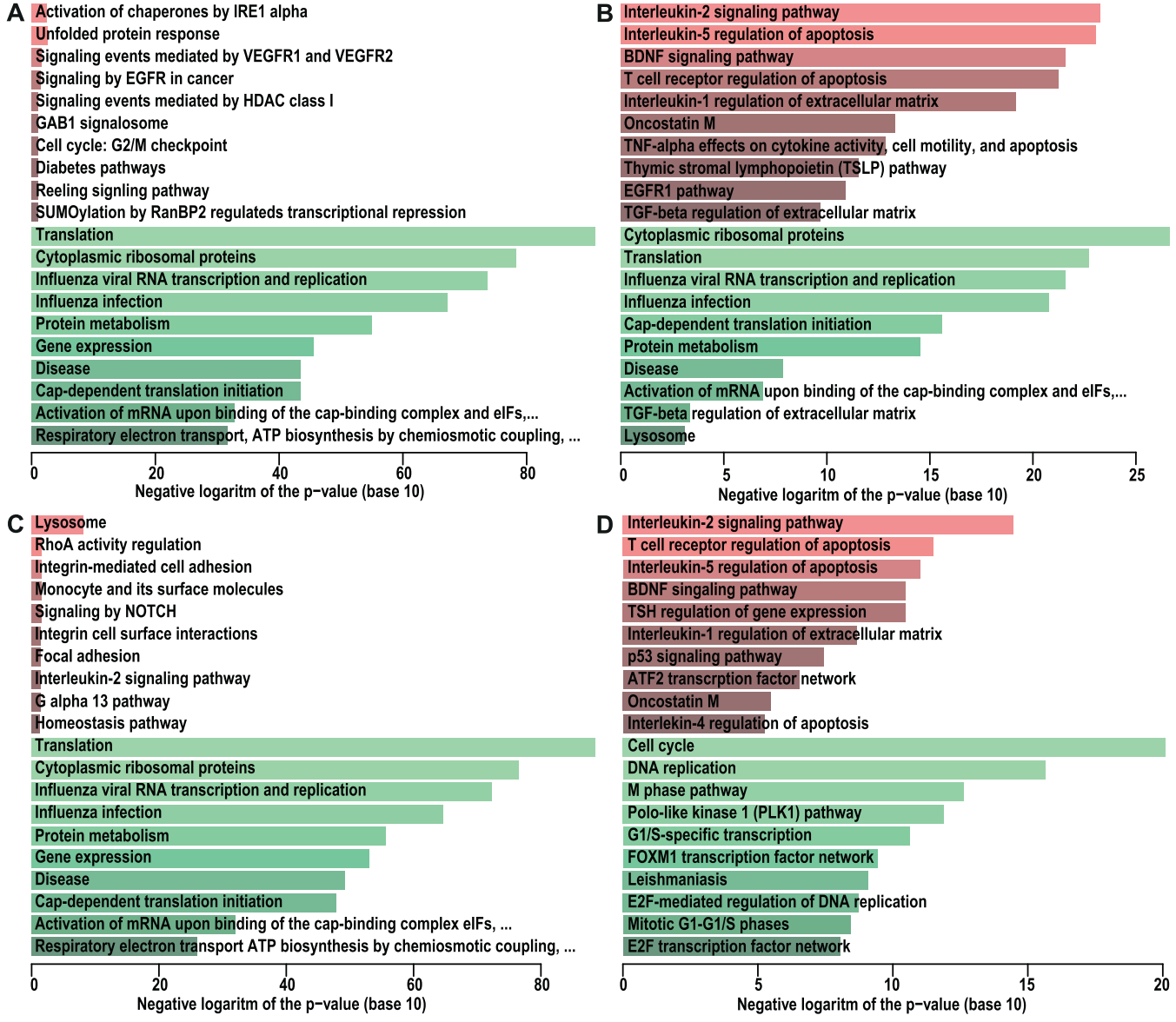

Fig. 6. Pathway enrichment analysis. Top ten significantly enriched BioPlanet pathways with DEGs in THP-1 macrophages (A, B) and MDM (C, D) treated with 20 μg/mL GO (A, C) or GNP (B, D) for 24 h. The graphs represent up-regulated (red) and down-regulated (green) DEGs in each pathway. The shown *p*-values are corrected for multiple testing. A full list of the enriched GO terms and the involved genes are available from Supplementary Table S3. (For interpretation of the references to colour in this figure legend, the reader is referred to the web version of this article).

also the most significant pathway upregulated in lung tissue of mice intratracheally exposed to a single dose of GO particles (Poulsen et al., 2021). UPR is a highly conserved cellular process and enables cells to manage endoplasmic reticulum (ER) stress toward restoring proteostasis. The UPR is increasingly recognized for its role in immune cell differentiation and function and in regulating immune and inflammatory responses (reviewed in (Grootjans et al., 2016)). Thus a future research direction may continue to exlpore whether GRM could induce a pathophysiolgical UPR and lead to pulmonary diseases. Furthermore, the lysosome pathway, which was perturbed by GO exposure in MDM, could be an interesting candidate for further studies since in macrophages, lysosomal proteolysis generates essential peptides that bind class II MHC molecules to create ligands for survey by the diverse antigen receptors of the T lymphocyte system (Watts, 2012). Moreover, antigen processing and presentation of exogenous peptide antigens were also prominent among the most down-regulated biological processes affected by GNP in MDM. Therefore, it could be relevant to address potential risks of GRM not only in healthy but also in infected lungs to understand if GRM could increase the susceptibility to or pathogenesis of lung infections or interfere with an effective innate immune response.

Down-regulated pathways were more similar between GO and GNP and mostly related to translation and cytoplasmic ribosomal proteins, which could indicate a slow down of cellular growth or replication.

Cell lines are frequently used for in vitro studies to achieve fast and reproducible results, but they may not fully recapitulate the behaviour of primary cells or physiological responses. For instance, a recent study revealed some alterations in chromosomal conformations and transcriptomes of THP-1 macrophages compared to primary MDMs (Liu et al., 2021). Indeed, the amount of common DEGs was mostly low for the 5 μg/mL exposure concentration but at 24 h of exposure to the high GRM concentrations (20 μg/mL) there was an increased overlap in the DEGs between THP-1 macrophages and MDM (Fig. S2). Here, the top 10 biological processes and pathways of the common DEGs did not reveal any novel interesting candidates (Supplementary Table S4) as compared to those described already for the two macrophage types (Figs. 4–6). For instance, there were multiple shared pathways between THP-1 macrophages and MDM such as IL-2 and IL-5 signalling pathways induced by GNP or responses in translation and gene expression that were down-regulated by GO in both cell types. Nevertheless, there were differences between differentiated THP-1 macrophages and MDM (e.g., GNP mostly affected transcription and protein targeting in THP-1 macrophages while in MDM, they activated cytokine and apoptotic processes), which could suggest that MDM might be more sensitive to NM exposure than THP-1 macrophages. In summary, we observed some overlap but also considerable differences in gene regulation from GRM exposure between primary MDM and THP-1 cell line and further validation in vivo would be required to understand whether the response of primary cells is more predictive.

4. Conclusion

In this study, we unveiled extensive effects of two physicochemically distinct GRM types (GO and GNP) on transcriptional response in primary human monocyte-derived macrophages and differentiated THP-1 macrophage cells. Despite the overlapping genes between the two GRM there is a high number of DEGs exclusively deregulated from each material type, which highlights that GRM is not a single class of material but that each GRM type is capable of mounting a highly material-specific molecular response. In addition to material characteristics, GRM impact on gene expression was also time- and dose-as well as macrophage type-dependent. It remains to be shown if the responses elicited in primary macrophages are more predictive than those in macrophage cell lines. In general, GNP elicited a stronger inflammatory and anti-apoptotic response at gene expression level than GO. However, long-term studies are warranted to understand if GNP exposure induces apoptosis in macrophages. Moreover, to better understand which characteristics are responsible for the observed differential transcriptional responses of GO and GNPs, future studies using GRMs that ideally differ in only one property would be required. Nevertheless, both GRM affected the expression of genes related to antigen processing and presentation which could indicate possible interference with essential functions of macrophages in innate immunity.

The biological processes and pathways identified in this study reflect acute toxicity responses but can guide future toxicity studies to better assess the long-term consequences of pulmonary GRM exposure. As such, it needs to be investigated if the identified mechanisms are of transient nature or whether they can result in long-term consequences to lung health. Importantly, such studies should be performed in appropriate models to adequately address the respective pathways, e.g., lung disease models to verify potential risks of GRM on lung infection or advanced lung models compatible with long-term exposure studies. In addition to the single exposure scenario investigated in this study, future research should further include repeated and prolonged exposure to GRM. This is highly relevant as exemplified in a recent study by Mukherjee et al. showing that repeated low-dose exposure of human bronchial cells (BEAS-2B) to GO can induce significant differences in the transcriptional response compared to a single high dose exposure (Mukherjee et al., 2020). Overall, the novel insights on the toxicity mechanisms of GO and GNP in macrophages are highly valuable for future research and a prerequisite to support the safe use of these promising materials.

CRediT authorship contribution statement

Daria Korejwo: Investigation, Writing – original draft, Visualization, Writing – review & editing. **Savvina Chortarea:** Investigation, Writing – original draft, Visualization, Supervision. **Chrysovalanto Louka:** Investigation. **Marija Buljan:** Investigation, Writing – original draft, Visualization. **Barbara Rothen-Rutishauser:** Conceptualization, Funding acquisition, Writing – review & editing. **Peter Wick:** Conceptualization, Funding acquisition, Project administration, Writing – review & editing. **Tina Buerki-Thurnherr:** Conceptualization, Writing – original draft, Visualization, Supervision, Project administration, Writing – review & editing.

Declaration of Competing Interest

The authors declare that they have no known competing financial interests or personal relationships that could have appeared to influence the work reported in this paper.

Data availability

The RNA sequencing data have been deposited in ArrayExpress database and are accessible via the ArrayExpress E-MTAB-10099 series accession number. Other data will be made available on request.

Acknowledgement

We are grateful to the staff at the Functional Genomics Centre Zurich for conducting RNAseq experiments and for providing ongoing technical support. We would like to thank Dr. Govind Gupta for sharing his knowledge on cell death/apoptosis mechanisms. The research leading to these results has received funding from the Swiss National Science Foundation (grant number 310030_169207) and The EU Horizon 2020 Framework Graphene Flagship project GrapheneCore2 (Grant Agreement No. 785219). DK and BRR acknowledge the support from the Adolphe Merkle Foundation.

Appendix A. Supplementary data

Supplementary data to this article can be found online at https://doi.

org/10.1016/j.impact.2023.100452.

References

Akhavan, O., Ghaderi, E., Akhavan, A., 2012. Size-dependent genotoxicity of graphene nanoplatelets in human stem cells. Biomaterials 33, 8017–8025.

Anders, S., Huber, W., 2010. Differential expression analysis for sequence count data. Genome Biol. 11. Epub ahead of print. https://doi.org/10.1186/gb-2010-11-10-r106.

Andrews, S.. FastQC - A Quality Control Tool for High Throughput Sequence Data. http://www.bioinformatics.babraham.ac.uk/projects/fastqc/. Babraham Bioinformatics.

Andrews, Simon, 2022. Babraham bioinformatics - FastQC a quality control tool for high throughput sequence data. Soil 5.

Barkan, T., 2019. Graphene: the hype versus commercial reality. Nature Nanotechnology 14. Epub ahead of print. https://doi.org/10.1038/s41565-019-0556-1.

Barlow, P.G., Clouter-Baker, A., Donaldson, K., et al., 2005. Carbon black nanoparticles induce type II epithelial cells to release chemotaxins for alveolar macrophages. Part Fibre Toxicol. https://doi.org/10.1186/1743-8977-2-11. Epub ahead of print.

Blank, F., Gerber, P., Rothen-Rutishauser, B., et al., 2011. Biomedical nanoparticles modulate specific CD4 + T cell stimulation by inhibition of antigen processing in dendritic cells. Nanotoxicology 5. Epub ahead of print. https://doi.org/10.3109/17435390.2010.541293.

Bray, N.L., Pimentel, H., Melsted, P., et al., 2016. Near-optimal probabilistic RNA-seq quantification. Nat. Biotechnol. 34 https://doi.org/10.1038/nbt.3519. Epub ahead of print.

Brown, D., Hutchison, G., Stone, V., et al., 2019. Proinflammatory effects of particles on macrophages and epithelial cells. In: Donaldson, K., Borm, P. (Eds.), Particle Toxicology. Taylor & Francis, pp. 183–196.

Brunner, T.J., Wick, P., Manser, P., et al., 2006. In vitro cytotoxicity of oxide nanoparticles: comparison to asbestos, silica, and the effect of particle solubility. Environ. Sci. Technol. https://doi.org/10.1021/es052069i. Epub ahead of print.

Cacialli, P., Mahony, C.B., Petzold, T., et al., 2021. A connexin/ifi30 pathway bridges HSCs with their niche to dampen oxidative stress. Nat. Commun. 12 https://doi.org/10.1038/s41467-021-24831-0. Epub ahead of print.

Cai, X., Dong, J., Liu, J., et al., 2018. Multi-hierarchical profiling the structure-activity relationships of engineered nanomaterials at nano-bio interfaces. Nat. Commun. 9. Epub ahead of print. https://doi.org/10.1038/s41467-018-06869-9.

Chaisson, M.J.P., Wilson, R.K., Eichler, E.E., 2015. Genetic variation and the de novo assembly of human genomes. Nat. Rev. Genet. 16, 627–640.

Chanput, W., Mes, J.J., Wichers, H.J., 2014 Nov. THP-1 cell line: an in vitro cell model for immune modulation approach. Int. Immunopharmacol. 23 (1), 37–45. https://doi.org/10.1016/j.intimp.2014.08.002. Epub 2014 Aug 14. PMID: 25130606.

Chen, E.Y., Tan, C.M., Kou, Y., et al., 2013. Enrichr: interactive and collaborative HTML5 gene list enrichment analysis tool. BMC Bioinform. 14. Epub ahead of print. https://doi.org/10.1186/1471-2105-14-128.

Clouter, A., Brown, D., Höhr, D., et al., 2001. Inflammatory effects of respirable quartz collected in workplaces versus standard DQ12 quartz: particle surface correlates. Toxicol. Sci. 90–98.

Creutzenberg, O., Oliveira, H., Farcal, L., et al., 2022. PLATOX: integrated in vitro/in vivo approach for screening of adverse lung effects of graphene-related 2D nanomaterials. Nanomaterials. 12 (8), 1254. https://doi.org/10.3390/nano12081254.

Czabotar, P.E., Lessene, G., Strasser, A., et al., 2014. Control of apoptosis by the BCL-2 protein family: Implications for physiology and therapy. Nat. Rev. Mol. Cell Biol. 15. Epub ahead of print. https://doi.org/10.1038/nrm3722.

Dobin, A., Gingeras, T.R., 2016. Optimizing RNA-seq mapping with STAR. Methods Mol. Biol. https://doi.org/10.1007/978-1-4939-3572-7_13. Epub ahead of print 2016.

Dobin, A., Davis, C.A., Schlesinger, F., et al., 2013. STAR: ultrafast universal RNA-seq aligner. Bioinformatics 29, 15–21.

Donaldson, K., Murphy, F.A., Duffin, R., et al., 2010. Asbestos, carbon nanotubes and the pleural mesothelium: a review of the hypothesis regarding the role of long fibre retention in the parietal pleura, inflammation and mesothelioma. Part Fibre Toxicol. https://doi.org/10.1186/1743-8977-7-5. Epub ahead of print.

Drasler, B., Kucki, M., Delhaes, F., et al., 2018. Single exposure to aerosolized graphene oxide and graphene nanoplatelets did not initiate an acute biological response in a 3D human lung model. Carbon N Y 137, 125–135.

Geim, A.K., Novoselov, K.S., 2007. The rise of graphene. Nat. Mater. 6, 183–191.

Graham, U.M., Jacobs, G., Yokel, R.A., et al., 2017. From dose to response: in vivo nanoparticle processing and potential toxicity. Adv. Exp. Med. Biol. 947, 71–100.

Grootjans, J., Kaser, A., Kaufman, R.J., et al., 2016. The unfolded protein response in immunity and inflammation. Nat. Rev. Immunol. 16 https://doi.org/10.1038/nri.2016.62. Epub ahead of print.

Hatakeyama, M., Opitz, L., Russo, G., et al., 2016. SUSHI: an exquisite recipe for fully documented, reproducible and reusable NGS data analysis. BMC Bioinform. 17. Epub ahead of print. https://doi.org/10.1186/s12859-016-1104-8.

Huang, R., Grishagin, I., Wang, Y., et al., 2019. The NCATS BioPlanet – an integrated platform for exploring the universe of cellular signaling pathways for toxicology, systems biology, and chemical genomics. Front. Pharmacol. 10, 445.

Hussell, T., Bell, T.J., 2014. Alveolar macrophages: plasticity in a tissue-specific context. Nat. Rev. Immunol. https://doi.org/10.1038/nri3600. Epub ahead of print.

Jing, X., Ren, D., Gao, F., et al., 2021. Gene deficiency or pharmacological inhibition of PDCD4-mediated FGR signaling protects against acute kidney injury. Acta Pharm. Sin. B 11. Epub ahead of print. https://doi.org/10.1016/j.apsb.2020.10.024.

Kong, W., Kum, H., Bae, S.H., et al., 2019. Path towards graphene commercialization from lab to market. Nat. Nanotechnol. 14, 927–938.

Kuleshov, M.V., Jones, M.R., Rouillard, A.D., et al., 2016. Enrichr: a comprehensive gene set enrichment analysis web server 2016 update. Nucleic Acids Res. 44. Epub ahead of print. https://doi.org/10.1093/nar/gkw377.

Li, Y., Liu, Y., Fu, Y., et al., 2012. The triggering of apoptosis in macrophages by pristine graphene through the MAPK and TGF-beta signaling pathways. Biomaterials 33. Epub ahead of print. https://doi.org/10.1016/j.biomaterials.2011.09.091.

Li, R., Guiney, L.M., Chang, C.H., et al., 2018. Surface oxidation of graphene oxide determines membrane damage, lipid peroxidation, and cytotoxicity in macrophages in a pulmonary toxicity model. ACS Nano 12, 1390–1402.

Liao, Y., Smyth, G.K., Shi, W., 2014. featureCounts: an efficient general purpose program for assigning sequence reads to genomic features. Bioinformatics 30, 923–930.

Liu, Y., Luo, Y., Wu, J., et al., 2013. Graphene oxide can induce in vitro and in vivo mutagenesis. Sci. Rep. 3, 3469.

Liu, X., Song, C., Yang, S., et al., 2020. IFI30 expression is an independent unfavourable prognostic factor in glioma. J. Cell. Mol. Med. 24. Epub ahead of print. https://doi.org/10.1111/jcmm.15758.

Liu, Y., Li, H., Czajkowsky, D.M., et al., 2021 Nov 5. Monocytic THP-1 cells diverge significantly from their primary counterparts: a comparative examination of the chromosomal conformations and transcriptomes. Hereditas. 158 (1), 43. https://doi.org/10.1186/s41065-021-00205-w.

Livak, K.J., Schmittgen, T.D., 2001. Analysis of relative gene expression data using real-time quantitative PCR and the 2-ΔΔCT method. Methods 25. Epub ahead of print. https://doi.org/10.1006/meth.2001.1262.

Mühlfeld, C., Ochs, M., 2009. Functional aspects of lung structure as related to interaction with particles. In: Particle-Lung Interactions, Second Edition.

Mukherjee, S.P., Kostarelos, K., Fadeel, B., 2018a. Cytokine profiling of primary human macrophages exposed to endotoxin-free graphene oxide: size-independent NLRP3 inflammasome activation. Adv. Healthcare Mat. 7. Epub ahead of print. https://doi.org/10.1002/adhm.201700815.

Mukherjee, S.P., Bondarenko, O., Kohonen, P., et al., 2018b. Macrophage sensing of single-walled carbon nanotubes via toll-like receptors. Sci. Rep. https://doi.org/10.1038/s41598-018-19521-9. Epub ahead of print.

Mukherjee, S.P., Gupta, G., Klöditz, K., et al., 2020. Next-generation sequencing reveals differential responses to acute versus long-term exposures to graphene oxide in human lung cells. Small. https://doi.org/10.1002/smll.201907686. Epub ahead of print.

Netkueakul, W., Korejwo, D., Hammer, T., et al., 2020. Release of graphene-related materials from epoxy-based composites: characterization, quantification and hazard assessment: In vitro. Nanoscale 12. Epub ahead of print. https://doi.org/10.1039/c9nr10245k.

Novoselov, K.S., Geim, A.K., Morozov, S.V., et al., 2004. Electric field in atomically thin carbon films. Science (1979). https://doi.org/10.1126/science.1102896. Epub ahead of print.

Oberdörster, G., Oberdörster, E., Oberdörster, J., 2007. Concepts of nanoparticle dose metric and response metric [1]. Environ. Health Perspect. 115 https://doi.org/10.1289/ehp.115-a290a. Epub ahead of print.

Oliveros, J.C.. VENNY. An Interactive Tool for Comparing Lists with Venn Diagrams. http://bioinfogp.cnb.csic.es/tools/venny/index.html.

Orecchioni, M., Jasim, D.A., Pescatori, M., et al., 2016. Molecular and genomic impact of large and small lateral dimension graphene oxide sheets on human immune cells from healthy donors. Adv. Healthcare Mat. 5, 276–287.

Poulsen, S.S., Bengtson, S., Williams, A., et al., 2021. A transcriptomic overview of lung and liver changes one day after pulmonary exposure to graphene and graphene oxide. Toxicol. Appl. Pharmacol. 410. Epub ahead of print. https://doi.org/10.1016/j.taap.2020.115343.

Riediker, M., Zink, D., Kreyling, W., et al., 2019. Particle toxicology and health - Where are we? Part Fibre Toxicol. https://doi.org/10.1186/s12989-019-0302-8. Epub ahead of print.

Sallusto, F., Cella, M., Danieli, C., et al., 1995. Dendritic cells use macropinocytosis and the mannose receptor to concentrate macromolecules in the major histocompatibility complex class II compartment: downregulation by cytokines and bacterial products. J. Exp. Med. 182, 389.

Scala, G., Kinaret, P., Marwah, V., et al., 2018. Multi-omics analysis of ten carbon nanomaterials effects highlights cell type specific patterns of molecular regulation and adaptation. NanoImpact. https://doi.org/10.1016/j.impact.2018.05.003. Epub ahead of print.

Schinwald, A., Murphy, F.A., Jones, A., et al., 2012. Graphene-based nanoplatelets: a new risk to the respiratory system as a consequence of their unusual aerodynamic properties. ACS Nano 6, 736–746.

Schinwald, A., Murphy, F., Askounis, A., et al., 2014. Minimal oxidation and inflammogenicity of pristine graphene with residence in the lung. Nanotoxicology 8, 824–832.

Schneider, V.A., Graves-Lindsay, T., Howe, K., et al., 2017. Evaluation of GRCh38 and de novo haploid genome assemblies demonstrates the enduring quality of the reference assembly. Genome Res. 27, 849–864.

Shin, J.H., Han, S.G., Kim, J.K., et al., 2015. 5-day repeated inhalation and 28-day post-exposure study of graphene. Nanotoxicology 9 (8), 1023–1031. https://doi.org/10.3109/17435390.2014.998306.

Szklarczyk, D., Morris, J.H., Cook, H., et al., 2017. The STRING database in 2017: quality-controlled protein-protein association networks, made broadly accessible. Nucleic Acids Res. 45. Epub ahead of print. https://doi.org/10.1093/nar/gkw937.

Tuguzbaeva, G., Yue, E., Chen, X., et al., 2019. PEP06 polypeptide 30 is a novel cluster-dissociating agent inhibiting αv integrin/FAK/Src signaling in oral squamous cell

carcinoma cells. Acta Pharm. Sin. B 9. Epub ahead of print. https://doi.org/10.1016/j.apsb.2019.10.005.
Warheit, D.B., Chang, L.Y., Hill, L.H., et al., 1984. Pulmonary macrophage accumulation and asbestos-induced lesions at sites of fiber deposition. Am. Rev. Respir. Dis. 129 (2), 301–310.
Watts, C., 2012. The endosome-lysosome pathway and information generation in the immune system. Biochim. Biophys. Acta, Proteins Proteomics 1824. Epub ahead of print. https://doi.org/10.1016/j.bbapap.2011.07.006.
Wick, P., Louw-Gaume, A.E., Kucki, M., et al., 2014. Classification framework for graphene-based materials. Angew. Chem. Int. Ed. 53, 7714–7718.
Witten, D.M., 2011. Classification and clustering of sequencing data using a poisson model. Ann. Appl. Stat. 5. Epub ahead of print. https://doi.org/10.1214/11-AOAS493.
www.graphene-flagship.eu.
Zerbino, D.R., Achuthan, P., Akanni, W., et al., 2018. Ensembl 2018. Nucleic Acids Res. 46. Epub ahead of print. https://doi.org/10.1093/nar/gkx1098.